ACS Catalysis

Research Article

pubs.acs.org/acscatalysis

Pt/Pd/Fe Trimetallic Nanoparticle Produced via Reverse Micelle Technique: Synthesis, Characterization, and Its Use as an Efficient Catalyst for Reductive Hydrodehalogenation of Aryl and Aliphatic Halides under Mild Conditions

Reza Abazari, Felora Heshmatpour,* and Saeed Balalaie*

Department of chemistry, Faculty of Science, K.N.Toosi University of Technology, P.O. Box 16315-1618, Tehran, 15418, Islamic Republic of Iran

ABSTRACT: The Pt/Pd/Fe trimetallic nanoparticle (Pt/Pd/Fe T-NP) was prepared using a water-in-oil microemulsion system of water/AOT/isooctane at room temperature. This nanoparticle (NP) was physically characterized by field emission scanning electron microscopy (FE-SEM), transmission electron microscopy (TEM), X-ray diffraction (XRD), and X-ray fluorescence (XRF) analyses. The said NP was used as catalyst for hydrodehalogenation (HDH) of halogenated organic compounds (HOCs), and its capability in hydrodechlorination (HDC) of chlorobenzene was compared with Pt/Pd, Pt/Fe, and Pd/Fe bimetallic nanoparticles (B-NPs) synthesized via the same method. The formation of mixed Pt/Pd/Fe ensembles results in an enhanced overall activity and reusability of HDC reaction, compared with Pd/Fe catalyst which acted as the best B-NP. Recycling experiments were examined for HDC of chlorobenzene. To get a maximum conversion of HDC, the reaction parameters like the effect of solvent, amounts of catalyst and ammonium formate were optimized. According to the results, HOCs, including electron-withdrawing and electron-donating substrates, were reduced smoothly. Finally, a mechanism for HDH reaction on the Pt/Pd/Fe catalyst surface was proposed.

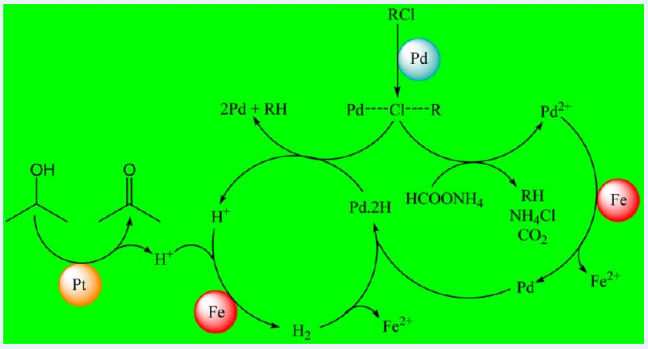

KEYWORDS: *reverse micelle, trimetallic nanoparticles, nano-catalyst, hydrodehalogenation, aryl chlorides*

1. INTRODUCTION

Halogenated organic compounds (HOCs) have been widely used in the chemical, petrochemical, and electronic industries. However, HOCs, especially chloroarenes have adverse effects because of their toxicity, deleterious environmental impact, and carcinogenic character which have been widely proved.[1−3] Therefore, growing interest has been attached to their destruction or conversion to harmless compounds. The combustion of HOCs is possible, but often results in the release of even more toxic compounds such as polychlorinated dibenzo-*p*-dioxins (PCDDs) and polychlorinated dibenzofurans (PCDFs).[4,5] For this end, several chemical degradation procedures have been suggested in the literature including the catalytic HDH process. HDH reaction is a nondestructive alternative technology with environmental potential in which HOCs wastes can be converted into products of commercial value.[6,7]

Zero-valent metal (ZVM) serves as a donor of electrons for promoting the reductive HDH of HOCs, as expressed by the following reaction (eq 1).[8,9]

$$M^0 + R{-}Cl + H^+ \rightarrow M^{2+} + R{-}H + Cl^- \quad (1)$$

However, the HDH reaction of some HOCs by monometallic NPs is not effective because of the slow rates and incomplete HDH reaction.[10,11] The nano zero-valent iron (NZVI), for example, has been frequently used because of its abundance, low cost, and non-toxicity.[12] However, it has some shortcomings, namely, low reactivity, and incomplete HDH reaction because of the formation of iron oxide or hydroxide over the surface of NZVI.[13] To overcome these shortcomings, in the past decade, a second catalytic metal has been incorporated with NZVI to form B-NPs that are exploited to hydrodehalogenate HOCs because of their higher efficiencies than a metal alone. Some bimetallic couples such as Pd/Re and Pd/Fe have been used in the HDH reactions, but with a limited success.[14,15] Among the catalytic metals, platinum and palladium have the most significant role in removal of halogen atom, especially chlorine, from HOCs. Also, since incorporation of a second, catalytic metal like Pd, Pt, Ni, Cu, or Zn onto the iron surface produces enhanced HDH reaction rates,[16−18] we have suggested the application of Pt/Pd/Fe T-

Received: July 30, 2012
Revised: December 11, 2012
Published: December 18, 2012

NP, which can act as one of the best catalysts in this process. The study of tri- and multimetallic catalysts is a new area of research applied for catalytic reforming[19,20] and other types of reactions,[21−23] but not for HDH reaction. These additives modify the activity, functionality, and selectivity of the catalyst.[24,25]

Most of these reactions are very frequently incomplete and need large amounts of catalyst, high heat, strongly basic conditions, and high pressure. In this context, a recent trend can be observed in the literature to evaluate progressively milder reaction conditions.[26,27] In the HDH reaction of HOCs, molecular hydrogen has been extensively used as a hydrogen source. For safety and simplicity of operation, a process without using molecular hydrogen is more advantageous. Using other hydrogen-transfer sources (e.g., metal hydrides, formic acid, alcohols, and ammonium formate), the process generally proceeds under safe and relatively mild conditions, which not only reduces energy cost but also suppresses the formation of undesirable byproducts.[28]

According to the literature, several methods have been proposed for metal NPs preparation. Much interest has recently been attached to the synthesis of uniform NPs as new catalysts for organic reactions. Since the size of NPs is controlled by the size of the droplet of the microemulsion (by use of the reverse micelles method) and since all micelles are similar in size, the prepared NPs have nearly uniform and homogeneous shape and same size.[29−31]

In this work, we aim to provide a proper catalytic system using Pt/Pd/Fe T-NP in the HDH reaction. The activity of this novel trimetallic nano-catalyst is compared with each pair of its constituent metal elements (i.e., comparison with bimetallic systems). Then, the reaction parameters are screened, and the results are evaluated. At last, the proposed reaction mechanism on Pt/Pd/Fe catalyst surface is discussed.

2. RESULTS AND DISCUSSION

2.1. Analysis of Catalyst NPs. Because of the high surface to volume ratio, metal NPs show unusual behavior compared to the bulk metals.[32] The property which is very evident for metal NPs after the addition of the reducing agent is their color change which indicates that the metal NPs are reduced. For instance, the color of Pt/Pd/Fe T-NPs was changed immediately from brownish-olive into black after the addition of hydrazine hydrate. This change in the color before and after reduction process is shown in Figure 1.

The preparation conditions affect the structure, shape (or morphology), and size distribution of the metal NPs. More to the point, preparation of NPs via the microemulsion gives a proper control of size and composition.[29] So, the reverse micellar technique is one of the most preferred candidates. The first question relating to the metal NPs is to investigate the aggregation state, size, and morphology. The surface morphology of all the synthesized samples was investigated by field emission scanning electron microscopy (FE-SEM), as shown in Figure 2. The FE-SEM images indicate that the synthesized NPs are approximately uniform and spherical in shape. Since the Pt/Pd, Pt/Fe, and Pd/Fe B-NPs have already been largely investigated by various analyses, only the FE-SEM analysis is used here to determine the surface morphology of these particles.

For further investigation of the Pt/Pd/Fe T-NPs, the structure, size, and elemental composition of the considered NPs were characterized using X-ray diffraction (XRD),

Figure 1. Digital photograph of Pt/Pd/Fe (1:1:2) T-NPs before (left-hand) and after (right-hand) reduction with hydrazine hydrate.

transmission electron microscopy (TEM), and X-ray fluorescence (XRF) analyses. Among the most frequently used techniques, TEM analysis is indispensable for the metal NPs studies. For TEM analysis, the synthesized sample was prepared by placing a drop of microemulsion solution onto the carbon coated copper TEM grids and drying it in air at room temperature. Figure 3 shows a typical TEM image and the particle size distribution histogram for the Pt/Pd/Fe T-NPs. The mean diameter and standard deviation were calculated by counting over 100 particles from a TEM image at ×450,000 magnification. The TEM image shows the existence of uniform, mono-disperse, and spherical particles, with a narrow size distribution of average diameter in the range of 14−24 nm.

X-ray diffraction is an effective method for investigation of the solid structure of NPs. To prepare the catalyst sample for XRD analysis, methanol was first added to the reverse micellar solutions for phase separation; then the mixture was centrifuged, and the catalyst was washed with methanol three times, and finally the obtained catalyst was dried at room temperature. Figure 4 shows the phase composition of Pt/Pd/Fe catalyst by the XRD analysis. The phase was identified by comparison with the Joint Committee on Powder Diffraction Standards (JCPDSs). The characteristic peaks for Pt (JCPDS number of card, 04-802; 2θ = 39.9°, 46.4°, 67.7°, 81.5°, and 86°) and those for Pd (JCPDS number of card, 05-0681; 2θ = 40°, 46.7°, 68°, 82°, 86°), marked by their indices ((111), (200), (220), (311), (222)) demonstrate the presence of the face-centered cubic (fcc) Pt and Pd crystallite. In contrast, the characteristic peak at 2θ = 44−45° confirms the existence of Fe^0 (α-Fe) with a body-centered cubic (bcc) structure (JCPDS number of card, 06-0696). The XRD pattern of the Pt/Pd/Fe catalyst in Figure 4 appears at 2θ values of 40.75°, 47.04°, 68.24°, 82.48°, and 86.92°, corresponding to the planes (111), (200), (220), (311), and (222) with fcc structure. In this XRD pattern, the five characteristic diffraction peaks are corresponding to the planes of Pt and Pd, but they are shifted to higher degrees, which is observable in the inset of this figure, indicating the formation of single-phase Pt/Pd/Fe alloy. As an example, despite the fact that the 2θ value of diffraction peak of Pd for the plane (111) was located at 40°, the 2θ value of diffraction peak of the Pt/Pd/Fe catalyst in the plane (111) in our XRD pattern is located at 40.75°, demonstrating that the

dx.doi.org/10.1021/cs300507a | ACS Catal. 2013, 3, 139−149

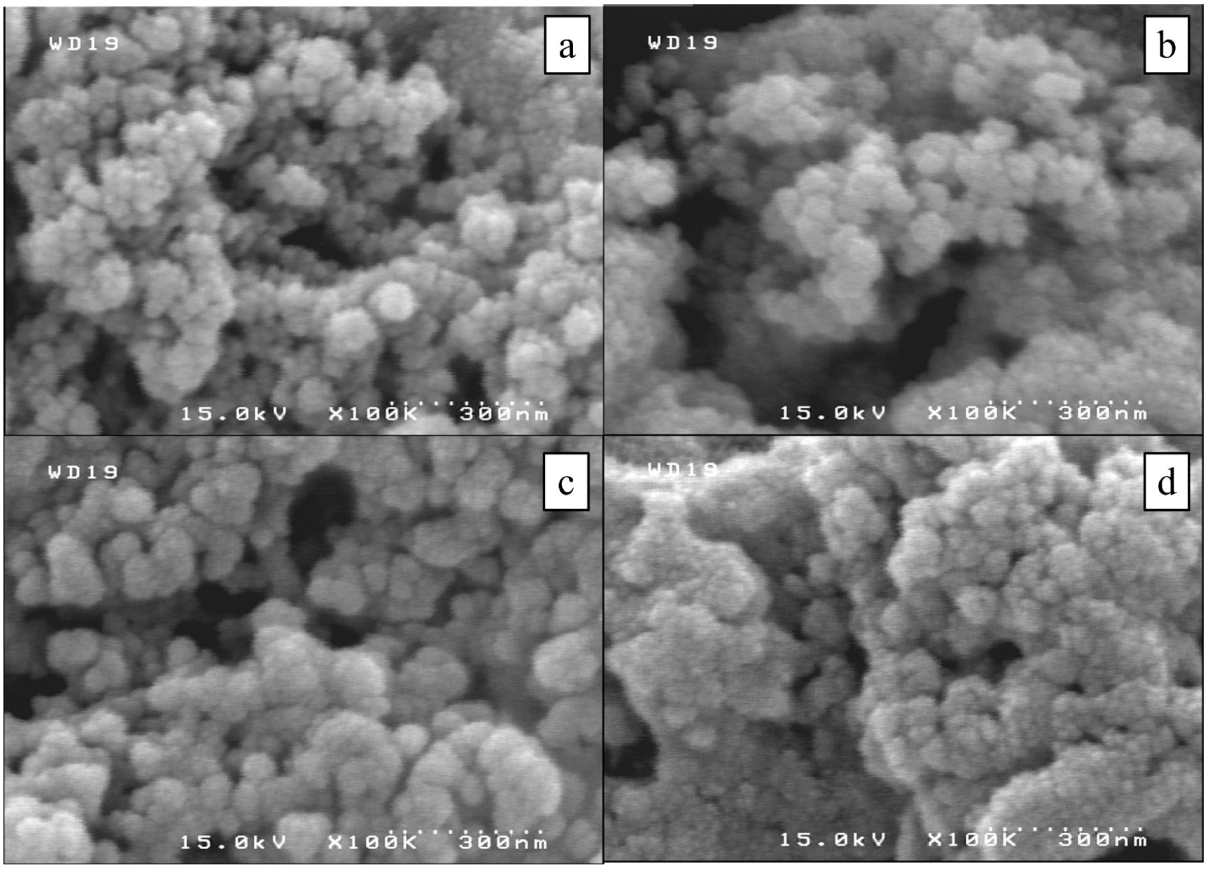

Figure 2. FE-SEM images of (a) Pd/Fe (1:1), (b) Pt/Fe (1:1), (c) Pt/Pd (1:1), and (d) Pt/Pd/Fe (1:1:2).

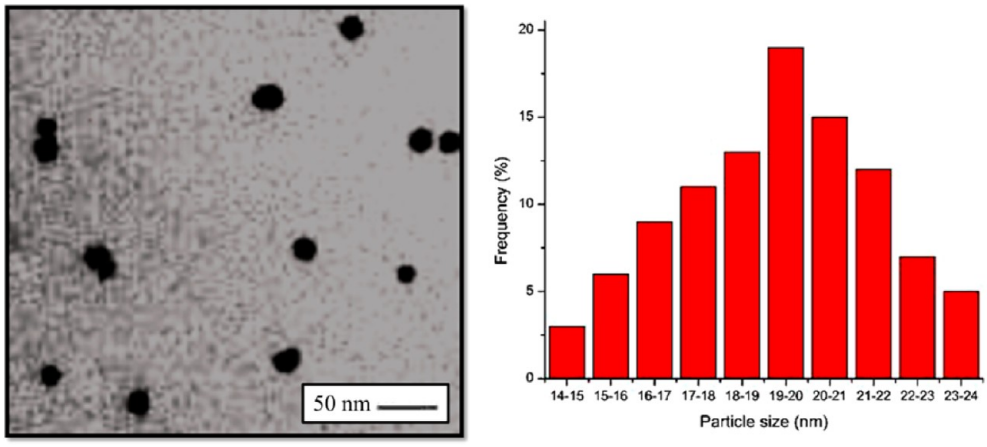

Figure 3. TEM image and the particle size distribution histogram of spherical Pt/Pd/Fe (1:1:2) T-NPs formed in the microemulsion.

formation of single-phase alloy causes the 2θ value to shift upward by $\Delta 0.75°$. Also, this issue indicates that a portion of Fe has entered the Pd and Pt lattice, forming the Pt/Pd/Fe trinary alloy phase. Since the radius of the Fe metal is smaller than that of the Pt and Pd, the 2θ values of the diffraction peaks of the Pt/Pd/Fe alloy are larger than those of the Pt and Pd particles, which follows Vegard's law.[33,34]

One of the major reasons for paying special attention to the alloy NPs (compared to both pure NPs and bulk alloys) lies in the fact that their chemical and physical properties can be tuned through the variation of the composition and atomic ordering and also the size of the particles. Therefore, because of the synergistic effect and unique atomic structures, alloy NPs have chemical, optical, thermal stability, mechanical, magnetic, surface structures, compositions, and segregation properties different from those of bulk alloys and pure NPs. Furthermore, these alloys have a higher strength-to-mass ratio than the commonly used materials. This especially makes them more powerful than the corresponding materials in their usage in the biomedical, optical, electronic industries, and particularly in the catalysts.[35−38]

Because no characteristic peaks of ferric oxide (2θ = 35.2−35.8°) were observed, the Fe^0 in Pt/Pd/Fe T-NP was not oxidized. Moreover, the broadening of the diffraction peaks indicates that the Pt/Pd/Fe NPs are small in size.

dx.doi.org/10.1021/cs300507a | ACS Catal. 2013, 3, 139−149

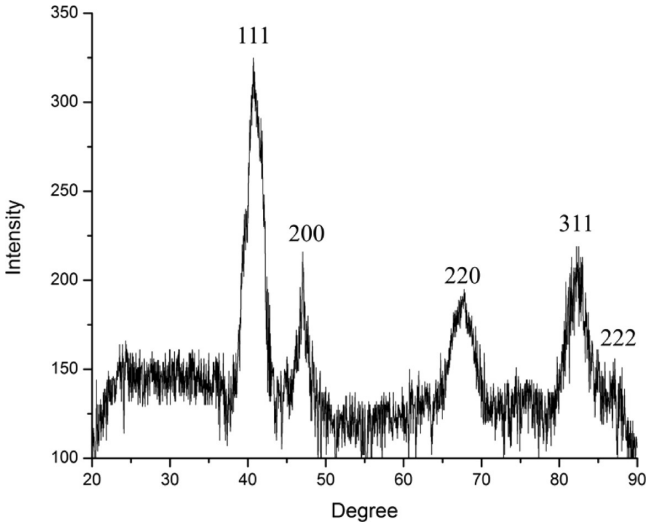

Figure 4. XRD spectrum of Pt/Pd/Fe (1:1:2) T-NPs synthesized in water/AOT/isooctane reverse micelles.

Using the Debye−Scherrer equation, the Pt/Pd/Fe T-NPs mean particle size (t) is calculated to be 17 nm as follows (eq 2).

$$t = k\lambda/\beta \cos\theta \quad (2)$$

The calculated size matches approximately the size observed from TEM image (t = 19.29 nm; with the size range average of 14−24 nm). In this equation, t is the mean particle size, k is the so-called shape factor, which usually takes a value of about 0.9, λ is the wavelength of X-ray source used in XRD, β is the full width in radians at half-maximum intensity (fwhm), and θ is the angle at maximum diffraction curve intensity.

XRF analysis is one of the most important techniques for the analysis of metals and trace elements, which is independent of the chemical form of the element. For this reason, to confirm the existence of Pt, Pd, and Fe species, Pt/Pd/Fe (1:1:2) T-NPs are examined by XRF analysis as the best catalyst for the HDH reaction; the element analysis shows the molar ratio of Pt:Pd:Fe is 21.00:23.15:43.07. This is very close to the designed molar ratio (theoretical value), suggesting that almost all elements have been involved into the final products.

In general, all the analyses have consistently shown fairly uniform NPs with small size. Recent literature has shown that synthesizing uniform NPs for organic reactions has attracted much attention.

2.2. Optimization of the Reaction Conditions. *2.2.1. Catalytic Testing.* First, optimization of the reaction conditions, that is, a series of solvents and catalysts (Pt/Pd, Pt/Fe, Pd/Fe, and Pt/Pd/Fe) with different molar ratios of the catalysts and appropriate amount of ammonium formate was investigated in the HDC reaction of chlorobenzene as a reactant. Recently, some studies on catalysis have been conducted to develop alternative reaction media so that synthetic procedures with a low environmental load can be achieved.[39] It is well-known that catalysts play key roles in the HDH reaction. In this context, a broad range of applications has been recognized for transition metal NPs, especially for noble metals of Group VIII which are known to promote the HDH reaction. In view of chemical stability and high catalytic reactivity, the metals in this group such as Pd and Pt have been considered to be a very good catalytic choice for most application, and mainly for the removal of a halogen atom, and especially the chlorine atom. One of the other advantages of the metals in Group VIII compared to other metals is their selectivity. For example, the rhodium metal not only cleaves the C−Cl bond but also causes the aromatic ring to be totally hydrogenated, whereas the Pd metal is merely limited to the hydrogenolysis of the C−Cl bond.[40] The Fe metal, also, regarding its abundance, low cost, non-toxicity, and benign environmental impact has been widely used in the reduction of the HOCs by the hydrogen gas arising from the corrosion on the iron surface.[12,41] But the reduction rate for the pure Fe metal tends to decrease with time (when exposed to air and aqueous solution) because of the formation of oxide layers that block the surface-active sites.[13,42]

The B-NPs, in which another metal is joined with the Fe metal, show higher catalytic activity than pure Fe metal, because of prevention of surface passivation by the presence of the other metal in the B-NP. For instance, in case of the Pd/Fe B-NP, not only does the Pd metal serve as catalyst absorbing H_2 generated from the iron corrosion, decomposing H_2 into atomic hydrogen (H*), and enhancing the rate of the HDH reaction, but it also prevents the oxidation of the iron surface when the particles are exposed to air.[43,44] Generally speaking, the reaction mechanism has already been investigated by the B-NPs as follows. One of the two metals in zero-valent form (with a negative reduction potential like, $Fe^0 \rightarrow Fe^{2+}$) produces molecular hydrogen by anodic corrosion, and the other metal with a relatively high (positive) reduction potential (such as $Pd^{2+} \rightarrow Pd^0$) serves as the reducing catalyst. Because of the above-mentioned reasons for the importance of the Pt, Pd, and Fe metals, we have compared the catalytic activities of the said metals as B- and T-NPs.

Figure 5 compares the activities of these metals (Pd, Pt, and Fe) as B- and T-NPs (Pd/Fe, Pt/Fe, Pt/Pd, and Pt/Pd/Fe) in

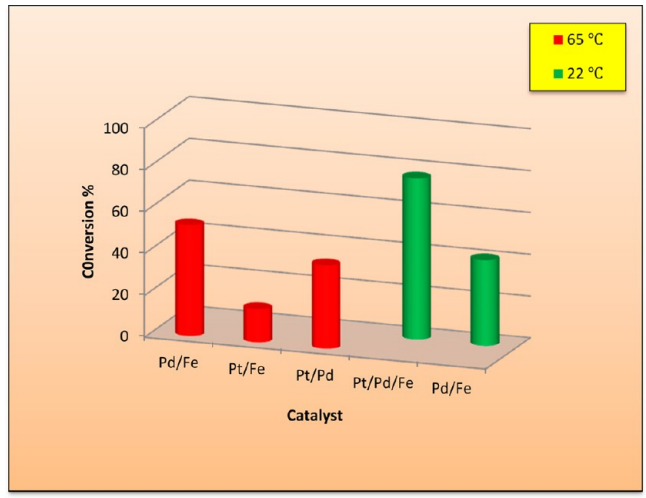

Figure 5. Comparison of the bimetallic (Pd/Fe, Pt/Fe, and Pt/Pd) and trimetallic (Pt/Pd/Fe) NPs activities on the hydrodechlorination reaction of chlorobenzene at 65 and 22 °C, respectively.

the HDC reaction of the chlorobenzene, with the reaction conversion of the said B-NPs at 65 °C as 53% (TON = 3220; TOF = 92 min^{-1}), 16% (TON = 971; TOF = 28 min^{-1}), 40% (TON = 2431; TOF = 69 min^{-1}) respectively and for the said T-NP at 22 °C as 77% (TON = 4681; TOF = 134 min^{-1}) in 35 min. It should be noted that the turn over numbers (TONs)

dx.doi.org/10.1021/cs300507a | ACS Catal. 2013, 3, 139−149

and the turn over frequencies (TOFs), which are defined as mmol product/mmol catalyst and mmol product/mmol catalyst per min, were calculated from the isolated yield. Worth mentioning, in the whole paper, the ratios of all B-NPs (Pt/Pd, Pt/Fe, and Pd/Fe) are adjusted to be 1:1, and the ratio of Pt/Pd/Fe T-NPs in this section is considered to be 1:1:1 (the latter may change in other sections). By keeping the other reaction parameters constant, catalytic activity of Pd/Fe (as the best B-NPs) was compared with that of the Pt/Pd/Fe (1:1:1) T-NPs at 22 °C for 35 min (Figure 5). According to the results, as the temperature decreased, the activity of Pd/Fe NP decreased with a conversion of 41% (TON = 2490; TOF = 71 min^{-1}). However, the rate and activity of the reaction was very favorable when Pt/Pd/Fe T-NP was applied with a conversion of 77% (TON = 4681; TOF = 134 min^{-1}). In general, the results show that the incorporation of Pd with Pt and Fe (as Pt/Pd/Fe T-NP) enhances catalytic activity, compared to the B-NPs of these metals. This high catalytic activity can be due to the charge transfer effect between different metals of this NP, which can cause to minimize the activation energy of the HDH reaction. This T-NP has been investigated using a new mechanism in Section 2.4.

2.2.2. Effect of the Solvent. In the present study, 10 different solvents, that is, MeOH, dimethylformamide (DMF), *n*-hexane, toluene, 1,4-dioxane, dimethylsulfoxide (DMSO), tetrahydrofuran (THF), CH_3CN, EtOH, and *i*-PrOH were examined to see their effect on the conversion. The effects of these solvents on the HDC reaction of chlorobenzene (with the catalyst ratio of Pt/Pd/Fe as 1:1:1 and 5 mmol ammonium formate at 22 °C in 35 min) are compared and listed in Figure 6. The maximum

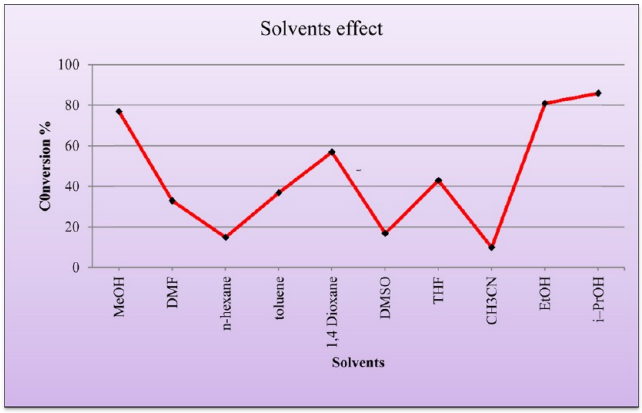

Figure 6. Effects of different solvents on the hydrodechlorination reaction of chlorobenzene as substrate at 22 °C for 35 min.

percentage of benzene conversion which can be obtained from various solvents is in the order, *i*-PrOH (TON = 5227; TOF = 149 min^{-1}) > EtOH (TON = 4923; TOF = 141 min^{-1}) > MeOH (TON = 4681; TOF = 134 min^{-1}) ≫ 1,4-dioxane (TON = 3462; TOF = 99 min^{-1}) > THF (TON = 2611; TOF = 75 min^{-1}) > toluene (TON = 2249; TOF = 64 min^{-1}) > DMF (TON = 2003; TOF = 57 min^{-1}) > DMSO (TON = 1031; TOF = 29 min^{-1}) > *n*-hexane (TON = 906; TOF = 26 min^{-1}) > CH_3CN (TON = 605; TOF = 17 min^{-1}).

Reaction in the more polar aprotic solvents, such as DMF, DMSO, and CH_3CN, formed only trace amounts of the desired products, especially for DMSO and CH_3CN. This might be attributed to the high coordination ability of these solvents which prevent the approach of substrate molecules to the metal center. A better result was obtained when we used the less polar solvent 1,4-dioxane. Using THF and toluene was not very successful and only 43% and 37% conversion was observed, respectively. A change in the solvent from one with less polarity to a nonpolar *n*-hexane solvent resulted in steep drop in the conversion which can be due to the poor solubility of ammonium formate that acts as hydrogen donor in the latter solvent. A review of these solvents showed that MeOH was still the best solvent in our catalytic system. Therefore, two other alcoholic solvents (EtOH and *i*-PrOH) were screened, and the results were more satisfactory. Among these three protic solvents, *i*-PrOH is the best solvent. Therefore, *i*-PrOH was chosen as the best solvent for the HDH reaction.

Because better results were obtained by using protic solvents, it can be inferred that the existing hydrogen in these solvents may have a role in the reduction of HOCs in the hydrogen transfer process on the catalyst surface. The corresponding mechanism will be discussed in more detail in the next subsections. As a result, the choice of solvents is considerably important to the catalytic reaction.

2.2.3. Amount of the Catalyst. Table 1, entries 1−5 shows the effect of varying the catalyst amount on the HDC reaction of chlorobenzene using *i*-PrOH as solvent with 5 mmol amount of ammonium formate and Pt/Pd/Fe (1:1:1) as catalyst. An increase (from 5.7×10^{-4} to 7.6×10^{-4} mmol) in the concentration of the catalyst did not result in the increase in the conversion (entries 1 and 2) and indeed, further increased amount of the catalyst lead to slight increase in the percentage of conversion (from 86% to 87%). When the catalytic amount decreased to 3.8×10^{-4} mmol, the product conversion was 84% (entry 3), which is a negligible decrease in relation to 3.8×10^{-4} mmol reduction in the amount of the catalyst (from 87% to 84%). Reducing the amount of the catalyst from 3.8×10^{-4} mmol to 2.85×10^{-4} mmol resulted in a decrease in the hydrodechlorinated conversion as 46% (TON = 5591; TOF = 160 min^{-1}) (entry 4). So, the minimum acceptable amount of the catalyst to be used in our system is 3.8×10^{-4} mmol (TON = 7658; TOF = 219 min^{-1}). To illustrate the importance and role of this catalyst in this reaction, an experiment was conducted in the absence of the said catalyst. According to the observations, only a slight conversion was obtained after 2 h (entry 5).

2.2.4. Amount of the Ammonium Formate. It was understood that HDC reaction of chlorobenzene took place smoothly in the reaction media with ammonium formate in the presence of a certain quantity of Pt/Pd/Fe T-NPs. Ammonium formate as catalytic transfer hydrogenating agent plays a key role in the hydrogen transfer. Representative results for the optimized amount of ammonium formate are shown in Table 1. When the amount of ammonium formate decreased from 5 to 4 mmol in 3.8×10^{-4} mmol of Pt/Pd/Fe (1:1:1) catalyst at 22 °C for 35 min, HDC proceeded smoothly with a slight increase in the conversion from 84% to 87% (entries 3 and 6). By reducing this amount to 3 mmol, the result was still satisfactory (entry 7). Lowering this amount to 2.5 mmol also allowed a relative reduction of chlorobenzene (entry 8). Therefore, we understood that the minimum amount of reducing agent compatible with 88% was 3 mmol in relation to the chlorobenzene. To highlight the importance and role of ammonium formate and the possible role of Pt metal in hydrogen transfer process, an experiment was conducted without these compounds (entries 9−11). In the absence of ammonium formate and in the presence of Pt/Pd/Fe catalyst

dx.doi.org/10.1021/cs300507a | *ACS Catal.* 2013, 3, 139−149

Table 1. Effect of the Amount of Catalyst and Ammonium Formate[a]

entry	catalyst (mmol ×10^{-4})	NH_4OCOH (mmol)	hydrodechlorination[b] %	TON[c]	TOF (min^{-1})[c]
1	5.7	5	86	5227	149
2	7.6	5	87	3967	113
3	3.8	5	84	7658	219
4	2.85	5	46	5591	160
5	none	5	trace		
6	3.8	4	87	7935	227
7	3.8	3	88	8029	229.5
8	3.8	2.5	79	7201	206
9	3.8	none	37	3372	96.5
10[d]	3.8	none	trace		
11[e]	3.8	none	0		

[a]Reaction condition: chlorobenzene (5 mmol), *i*-PrOH (3 mL), 22 °C, 35 min. [b]Hydrodechlorination was determined by GC, which was then compared to an internal standard (*n*-Octane). [c]Calculated from the isolated yields by fractional distillation (TON = mmol product/mmol catalyst; TOF = mmol product/mmol catalyst per min). [d]Performed by Pd/Fe catalyst with *i*-PrOH as solvent at 2 h. [e]1,4-Dioxane as solvent in the presence of Pt/Pd/Fe catalyst at 2 h.

and the solvent *i*-PrOH, a conversion of 37% was obtained, which can be accounted for by the fact that the hydrogen ions arising from the dehydrogenation of *i*-PrOH on Pt particles surface are likely to make reduced HOCs (entry 9). To prove this, an experimental was conducted, in which Pd/Fe was used as catalyst (in place of the Pt/Pd/Fe) without ammonium formate in the solvent *i*-PrOH, and so a slight conversion was provided after 2 h (entry 10). Moreover, when the protic solvent was replaced with a polar aprotic solvent in the presence of Pt/Pd/Fe catalyst and in the absence of ammonium formate, no results were obtained in the reaction after 2 h (entry 11). These results indicate the importance of both ammonium formate and the metal Pt in the hydrogen transfer process into HOCs.

2.2.5. Effects of Molar Ratio of the Three Metals, Pd, Pt, and Fe. Figure 7 shows the effect of changing molar ratios of

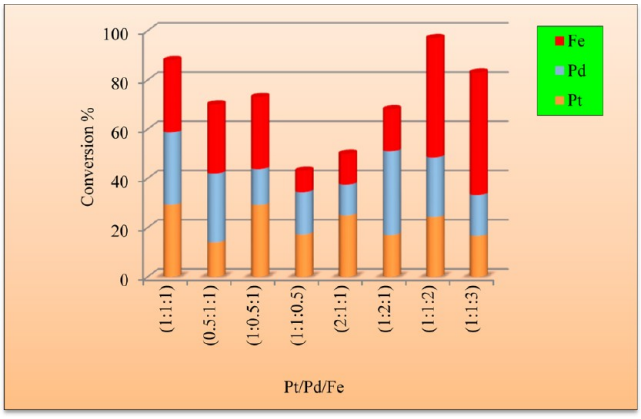

Figure 7. Effects of elemental ratio in the Pt/Pd/Fe T-NPs on the hydrodechlorination reaction of chlorobenzene at 22 °C for 35 min.

these three metal ions in the HDC reaction of chlorobenzene at 22 °C for 35 min. We have determined that a 1:1:2 molar ratio of Pt, Pd, and Fe, respectively, gave the best catalyst combination in three metals with a conversion of 97% (TON = 8848; TOF = 253 min^{-1}). Lowering only one of these metal ions in a single process (0.5:1:1, 1:0.5:1, and 1:1:0.5), a decrease in the reaction rate and activity was obtained with 70%, 73%, and 43% conversions, respectively (TONs = 6383, 6660, and 3920; TOFs = 182, 190, and 112 min^{-1} respectively). Also, an increase in the amount of either Pt or Pd in relation to the other two metals (2:1:1 and 1:2:1) lead to 50% and 68% conversions, respectively (TONs = 4557 and 6201; TOFs = 130 and 177 min^{-1} respectively). When the molar ratio of Fe became three times larger than the other two metals (1:1:3), the conversion was reduced from 97% to 83% (TON = 7569; TOF = 216 min^{-1}).

It can be concluded that the optimized conditions for the HDC reaction of chlorobenzene were as follows: 3.8 × 10^{-4} mmol Pt/Pd/Fe catalyst with the molar ratio of 1:1:2 and 3 mmol ammonium formate in *i*-PrOH solvent at 22 °C for 35 min. Finally, we used these optimized conditions for investigation of a series of aryl and aliphatic halides compounds.

2.2.6. Reusability of the Catalyst. The practical application of catalysts to the HDH reaction of HOCs is always accompanied by the problem of the deactivation of the catalyst. Therefore, in practical use, developing catalysts that keep their catalytic activity for a prolonged time is a major problem.[28,45,46] Great importance is attached to these aspects, and so a number of examples exist in the literature that report recycling experiments.[47−49] In the present work, we have studied the potential recycling process of Pt/Pd/Fe (1:1:2) and Pd/Fe (1:1) (as our best B-NP in this study) catalysts. To evaluate the catalytic life of the said catalysts, the HDC reaction of chlorobenzene was repeated several times with the catalyst recovered after each reaction. The catalytic stability of these two catalysts up to six runs at 22 °C is shown in Figure 8. Before the next run, the catalyst system was easily separable, by centrifugation, from the reaction mixture by decantation of the liquid phase, and then the catalyst was washed with diethyl ether, dried at 60 °C, and was used for a new run. Each reaction was run for 35 min, which was the necessary time for completing the reaction. In case of Pd/Fe catalyst, when this treatment was performed, a significant decrease in the catalytic activity of Pd/Fe was observed after each run, so that by the second run, the activity decreased with a conversion of 54% to 31%. The catalytic activity decreased gradually so that in the sixth run the conversion was 7% (TON = 635; TOF = 18 min^{-1}). These results can be attributed to the decreasing amount of Pd/Fe catalyst versus the number of cycles, which shows that the contribution of Pd/Fe catalyst in the HDC reaction of chlorobenzene is important. On the other hand, the feature of the HDC reaction with Pt/Pd/Fe (1:1:2) is different so that almost no loss of catalytic activity was observed after five

dx.doi.org/10.1021/cs300507a | *ACS Catal.* 2013, 3, 139−149

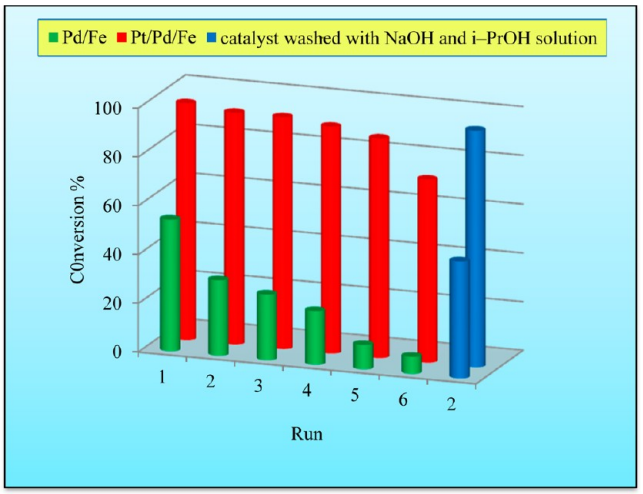

Figure 8. Comparison of conversion and reusability of Pd/Fe (1:1) and Pt/Pd/Fe (1:1:2) NPs as catalysts in the hydrodechlorination of the chlorobenzene at 22 °C for 35 min.

runs. However, in the sixth run, a little decrease in the conversion resulted (TON = 6839; TOF = 195.5 min^{-1}), that is, a 22% decrease compared with the first run. These results show that the amount of leached catalyst after each run is low.

Another reason for such a gradual decrease in the catalytic activity is probably due to the accumulation of produced salts such as NH_4Cl on the catalyst surface and/or surface deactivation with the produced H−Cl.[40,50,51] The accumulated NH_4Cl on the catalytic surface can be removed by washing with diethyl ether or water. It has been reported that in the HDH reaction, the addition to bases such as NaOH and NH_3 is effective in suppressing the deactivation and causes the catalysts to restore the activity, since the halogen ions responsible for the poisoning are removed from the catalyst surface.[50,52] In view of this, in our experiment, after the Pd/Fe catalyst was used in the first run, it was washed with a solution of NaOH (at a NaOH-to-catalyst molar ratio of 2.0) in 2-propanol (5 mL) at room temperature for 15 min. The conversion after this treatment decreased a little from 54% to 48% which is probably because the catalyst surface became cleaner and/or reduced, as shown in Figure 8 in a blue bar. Similar action was performed for Pt/Pd/Fe catalyst after the first run, for which the results show no loss of catalytic activity, as shown in Figure 8 in a blue bar. In short, this reveals the excellent stability and recyclability of the novel catalyst Pt/Pd/Fe (1:1:2).

2.3. Hydrodehalogenation of Aryl and Aliphatic Halides. To study the scope of HDH reaction, the HDH of several HOCs was investigated under the same experimental conditions. Under the optimized reaction conditions, a range of functionalized substituents, including OMe, CHO, NO_2,

Table 2. Hydrodehalogenation of Aryl and Aliphatic Halides Using Pt/Pd/Fe Catalyst[a]

entry	starting material	product	hydrodehalogenation[c] %	TON[e]	TOF (min^{-1})[e]
1[b]	bromoacetic acid	acetic acid	100	5683	284
2[b]	chloroacetic acid	acetic acid	95	7932	396.5
3[b]	2-chloro-2-methylbutane	2-methylbutane	91	7509	375.5
4[b]	ethyl-4-chloroacetoacetate	ethyl acetoacetate	94	9766	488
5	Iodobenzene	benzene	100[d]	5030	144
6	bromobenzene	benzene	100[d]	6537	187
7	chlorobenzene	benzene	97[d]	8848	253
8	4-bromoaniline	aniline	99	7047	201
9	4-bromophenol	phenol	95	6794	194
10	4-bromoanisole	anisole	97	7317	209
11	2-chloroaniline	aniline	91	8730	249.5
12	4-chloroaniline	aniline	95	9116	260.5
13	2-chlorophenol	phenol	89	8564	245
14	4-chloro-3-methylphenol	3-methylphenol	81	8075	231
15	5-bromo-2-hydroxybenzaldehyde	2-hydroxybenzaldehyde	93	7428	212
16	2-bromobenzaldehyde	benzaldehyde	96	7237	207
17	3-bromobenzaldehyde	benzaldehyde	97	7315	209
18	4-bromobenzaldehyde	benzaldehyde	100	7540	215.5
19	4-chlorobenzaldehyde	benzaldehyde	93	9227	264
20	3-chlorobenzoic acid	benzoic acid	99	10151	290
21	3,5-dichlorobenzoic acid	benzoic acid	93	7811	223
22	2,5-dichloroaniline	aniline	73	5513	157.5
23	4,5-dichloroaniline	aniline	77	5815	166
24	2,6-dichloroaniline	aniline	71	5362	153
25	2,6-dichloro-4-nitroaniline	4-nitroaniline	75	6576	188
26	1,4-dibromobenzene	benzene	98[d]	4265	122
27	1,2-dichlorobenzene	benzene	78[d]	5440	155.5
28	1,4-dichlorobenzene	benzene	83[d]	5794	165.5
29	2-chloropyridine	pyridine	91	8329	238

[a]Reaction condition: starting material (5 mmol), catalyst (3.8×10^{-4} mmol), NH_4OCOH (3 mmol), *i*-PrOH (3 mL), 22 °C, 35 min. [b]At 22 °C for 20 min. [c]All compounds were characterized by GC. [d]Compared to an internal standard (*n*-Octane, entries 5−7, and 26−28). [e]Calculated from the isolated yields by silica gel column chromatography (entries 8−25, and 29) and fractional distillation (entries 1−7, and 26−28), (TON = mmol product/mmol catalyst; TOF = mmol product/mmol catalyst per min).

dx.doi.org/10.1021/cs300507a | *ACS Catal.* 2013, 3, 139−149

COOH, OH, NH_2, I, Br, and Cl were employed with good to excellent conversions. The corresponding results are listed in Table 2, entries 1−29. In the first step, reduction of a series of aliphatic compounds was investigated for 20 min (the necessary time to complete the reaction) with excellent result (entries 1−4). In the next step, the influence of halide was studied. It is clear that aromatic chlorides show much less reactivity than aromatic bromides and iodides, the HDC of aromatic chlorides is an incomplete methodology, and few effective general methods have been reported in the literature.[53,54] Thus, the development of new HDC methods is still of particular interest. In our work, chlorobenzene was efficiently reduced to benzene in 35 min (entry 7); in contrast, bromobenzene and iodobenzene were reduced to benzene in 20 min (entries 5 and 6). The reactivity of halogens was found to be in the general order of I > Br > Cl, as indicated in various reduction reactions.[55,56]

As illustrated in entries 8−25, HDH reaction of bromo and chloro arenes bearing aniline, aldehyde, benzoic acid, anisole, methyl, nitro, or phenol groups occurs smoothly in good to near quantitative conversions. As reported by some papers in the literature, because of the much higher bond strength of C−Cl in the aromatic ring, chlorinated aromatics are generally recalcitrant in HDC reaction, compared to chlorinated aliphatics.[57] However, in our catalytic system, chlorinated aryl compounds were reduced smoothly. Electron-donating (runs 8−14 and 22−25) as well as electron-withdrawing (runs 15−21) substituents were readily hydrodehalogenated under similar conditions to give the corresponding reduced products with high conversion ranging from 71% to 100%, although better results were obtained from electron-withdrawing groups.

HDH reaction of dibromobenzene (entry 26) and dichloroarenes (entries 21−25, 27 and 28) took place smoothly with the mentioned catalytic system so that benzene, aniline, and benzoic acid were given with excellent conversions. The rate of these reductions was however slower than those noted with mono-chloroarenes. Compared with less hindered substrates, the more hindered substrates caused to decrease the reaction rate because of a slower oxidative-addition step. In our experiment, for the very same reason as mentioned above, the substrates 2,5-dichloroaniline, 2,6-dichloroaniline, and 2,6-dichloro-4-nitroaniline led to the HDC product with almost lower conversions in 35 min (entries 22, 24, and 25). Lastly, the HDC of 2-chloropyridine resulted with 91% conversion (entry 29). For this catalyst system, TONs and TOFs were relatively higher than some of the other systems. In conclusion, the Pt/Pd/Fe T-NP is an efficient catalyst on the HDH reaction of aryl and aliphatic halides for both electron-withdrawing and electron-donating groups.

2.4. Hydrodehalogenation Reaction Mechanism on Pt/Pd/Fe Catalyst Surface. Several mechanisms for the HDH process have already been suggested, and some general tendencies emerge. Optimization of the reaction condition can always help in determining the role and contribution of metal NPs in the catalytic cycle, especially the B- and T-NPs, in the reaction path. For example, in our proposed system, when the molar ratio of Fe was twice as large as the ratio of Pt and Pd, the reaction condition was improved, and so it is understood that Fe can be more employed in this catalytic cycle. Since iron is the most available and commonly used metal, using larger amounts of Fe than Pd and Pt, which are two expensive noble metals, in the present catalyst (Pt/Pd/Fe (1:1:2)) can be considered as a valuable advantage of our system. Figure 9 suggests a mechanism for the HDH reaction on the Pt/Pd/Fe (1:1:2) catalyst surface. This mechanism

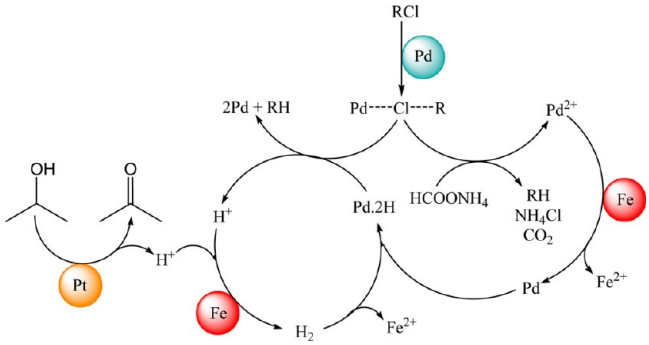

Figure 9. Proposed mechanism for catalytic cycle of hydrodehalogenation reaction on the Pt/Pd/Fe (1:1:2) T-NPs surface.

shows that the reaction proceeds by two different paths that cause a cleavage in the R−Cl bond so as to form R−H. For reduction of HOCs to occur, both HOCs and H_2 must be adsorbed to make it possible to dissociate both C−Cl and H−H bonds on the catalyst surface.[58] Many studies indicate that the breaking of the C−Cl bond is involved in the rate determining step.[59,60] In the first step of our proposed mechanism, Pd can cause the C−Cl bond to weaken in an oxidative-addition step. In one of the two above-mentioned paths, ammonium formate, which acts as the hydrogen source, can result in the reduction of HOCs; besides, the additional amount of Fe can make Pd metal regenerate once again in an electron transfer process with the standard potential of 0.238 V as follows,[61] ((eqs 3−5).

$$Pd^0 + RCl \rightarrow Pd\cdots Cl\cdots R \quad (3)$$

$$Pd\cdots Cl\cdots R + NH_4COOH \rightarrow RH + NH_4Cl + CO_2 + Pd^{2+} \quad (4)$$

$$Fe^0 + Pd^{2+} \rightarrow Pd^0 + Fe^{2+} \quad (5)$$

In the other path of our mechanism, the hydrogen ion can arise from the *i*-PrOH solvent on the surface of the Pt metal. It has already been suggested that dehydrogenation of 2-propanol on the Pt particles' surface can cause the production of active hydrogen ions.[62,63] Because of the corrosion of Fe metal resulting from the low standard redox potential (−0.44 V) of the Fe/Fe^{2+} couple, the released hydrogen ions in the catalytic cycle can lead to the emergence of molecular hydrogen (eq 6).[64]

$$Fe^0 + 2H^+ \rightarrow Fe^{2+} + H_2 \quad (6)$$

In the next step, the regenerated Pd and the produced H_2 in the catalytic cycle are combined to form a transitional compound Pd·2H. It is well-known that atomic hydrogen (H*) can be formed from the dissociation of H_2 on the Pd surface when molecular hydrogen is present.[65] Because the Pd metal has a very low hydrogen overpotential compared to the Fe metal, H_2 dissociation on the Pd surface can be simply catalyzed with a low activation barrier ($\leq$8.4 kJ mol^{-1}).[66] Therefore, the produced atomic hydrogen (second path) on the Pd surface caused to reduce the HOCs (eqs 7 and 8).

$$Pd^0 + H_2 \rightarrow Pd\cdot 2H^* \quad (7)$$

dx.doi.org/10.1021/cs300507a | *ACS Catal.* 2013, 3, 139−149

$$Pd\cdots 2H^{*} + Pd\cdots Cl\cdots R \rightarrow RH + H^{+} + Cl^{-} + 2Pd^{0} \quad (8)$$

Finally (after completion of reaction), the iron ions produced in the catalytic cycle could be again achieved by adding 0.1 mmol of sodium borohydride (at a BH_4^--to-Fe^{2+} molar ratio of 2.0) into the separated catalyst. This caused the reduction and regeneration of Fe^{2+} on the Pt/Pd/Fe T-NPs surface. This electron transfer from the reducing agent (BH_4^-) to Fe^{2+} were represented according to the following equation,[67] (eq 9).

$$Fe^{2+} + 2BH_4^- + 6H_2O \rightarrow Fe^0 + 2B(OH)_3 + 7H_2 \quad (9)$$

To prove again the regeneration of Fe^{2+} into Fe^0 using $NaBH_4$, after separation of the catalyst from the reaction mixture, two experiments were separately conducted. Case (I) was performed without regeneration of the catalyst while in case (II) the separate catalyst was added to the $NaBH_4$ (0.1 mmol) and methanol solution (3 mL) at room temperature for 30 min. In both cases, 4-bromoanisole was used as the substrate. The reaction yields for case (I) and (II) were 87% (TON = 6508; TOF = 187 min^{-1}) and 98% (TON = 7321; TOF = 211 min^{-1}) respectively, hence showing the effect of $NaBH_4$ on the catalytic activity. However, since the effect of this amount does not make any considerable difference, Pd/Fe (1:1) was used as the catalyst while other reaction conditions were kept constant. In this context, the reaction yields for case (I) and (II) were 24% (TON = 1764; TOF = 52 min^{-1}) and 66% (TON = 4944; TOF = 142 min^{-1}), respectively, thereby showing the importance of the regeneration of the catalyst through $NaBH_4$.

3. SUMMARY AND CONCLUSION

In conclusion, a simple method for preparing metal NPs (Pt/Pd, Pt/Fe, Pd/Fe, and Pt/Pd/Fe) has been adopted based on the reverse micelle technique. Surface morphology of all the synthesized NPs was shown using FE-SEM analysis. Besides, the size, structure and elemental composition of Pt/Pd/Fe (1:1:2) T-NPs as the best catalyst have been further investigated using TEM, XRD, and XRF analyses, in addition to FE-SEM analysis. In the HDC process of chlorobenzene, activity of bimetallic (Pt/Pd, Pt/Fe, and Pd/Fe) and trimetallic (Pt/Pd/Fe) NPs has been compared. This T-NP has much higher catalytic activity for HDC reaction than corresponding B-NPs. Using *i*-PrOH as solvent and the catalyst (Pt/Pd/Fe) and ammonium formate amounts equaling 3.8 mmol $\times 10^{-4}$ and 3 mmol, respectively, the optimum conditions for this reaction have been obtained. The best molar ratios of these three metals as Pt, Pd, and Fe are 1:1:2, respectively. This catalyst is easily separable and recyclable in five successive runs with little reduction in catalytic efficiency. As the results show, in the presence of the said ternary metallic catalyst, the HDH process takes place smoothly using aqueous ammonium formate with high efficiency, which causes a reduction in the HOCs with a safe and clean detoxification protocol. Under these conditions, electron neutral, rich, or poor HOCs can be mildly and rapidly hydrodehalogenated at room temperature. Finally, by our proposed mechanism, the importance and role of each of these metals (Pt, Pd, and Fe) in the HDH reaction has been investigated. To the best of our knowledge, this is the first report on the use of Pt/Pd/Fe T-NP, synthesized via reverse micelles, in the HDH reaction of HOCs.

4. EXPERIMENTAL SECTION

4.1. Materials. The following chemicals were used in the synthesis procedure: hexachloroplatinic(IV) acid hexahydrate ($H_2PtCl_6{\cdot}6H_2O$ 99.9%, Alfa), palladium(II) acetate ($Pd(OAc)_2$ ≥99%, Merck), iron(II) chloride tetrahydrate ($FeCl_2{\cdot}4H_2O$, Merck), as precursor salts; dioctyl sulfosuccinate sodium salt (aerosol-OT, AOT 98%, Aldrich) as a surfactant; hydrazine hydrate ($N_2H_4.H_2O$ ≥99%, Merck) as a reducing agent; isooctane (≥99%, Merck) as the oil phase; ammonium formate (97%, Acros) as a hydrogen donor, methanol (≥99.9%, Merck) as a washing agent and solvent; and water used in the experiments was deionized (DI) and doubly distilled prior to use as the aqueous phase in reverse micelle system. Substrates were purchased from Merck Company, and were used without further purification or drying.

4.2. Characterization. The shape (or morphology), size, crystal structure, and elemental composition of the Pt/Pd/Fe T-NPs were characterized by FE-SEM, TEM, XRD, and XRF analyses. Also, the surface morphology of all the synthesized B-NPs (Pt/Pd, Pt/Fe, and Pd/Fe) was characterized by the FE-SEM analysis only. FE-SEM images were obtained on a Hitachi S-1460 field emission scanning electron microscope using accelerating voltage of 15 kV. TEM measurement for Pt/Pd/Fe was performed on a Philips model EM-208S instrument operated at an accelerating voltage of 100 kV. Usually more than 100 particles from different parts of the grid were used to estimate the average size and size distribution of particles. XRD analysis of the Pt/Pd/Fe T-NPs was carried out using a Philips diffractometer (Model TM-1800). Nickel filtered Cu-Kα radiation source was used to produce X-ray (λ = 1.542 Å), and scattered radiation was measured with a proportional counter detector at a scan rate of 4°/min. The scanning angle was from 20° to 90°, operating at a voltage of 40 kV applying potential current of 30 mA. The elemental composition of the Pt/Pd/Fe T-NPs was determined by Philips model PW-1480 Fluorescence Spectrometer (XRF) operating at 4 kW with Rh Kα radiation source. Gas Chromatography (GC) data was recorded on a GC Shimadzu 14B with a SA13-5 capillary column (phenyl methyl siloxane, 30 m × 320 mm ×0.25 mm).

4.3. Preparation of the Catalyst. *4.3.1. Preparation of the Pd/Fe, Pt/Fe, and Pt/Pd B-NPs.* Pd/Fe NP was synthesized as follows, while the same procedure is true for the other NPs. Three microemulsions with different aqueous phases containing 0.01 mmol $Pd(OAc)_2$, 0.01 mmol $FeCl_2{\cdot}4H_2O$, and 0.7 mmol $N_2H_4{\cdot}H_2O$ were prepared (note that each microemulsion was formed with 0.1 M AOT concentration and a given amount of isooctane as the oil phase). Then, microemulsion A (containing 0.01 mmol $Pd(OAc)_2$) was mixed to microemulsion B (containing 0.01 mmol $FeCl_2{\cdot}4H_2O$) which is hereafter called microemulsion I. After mechanical agitation for about 30 min, microemulsion C (containing 0.7 mmol $N_2H_4{\cdot}H_2O$) was mixed in the microemulsion I. The reaction time was maintained for 1 h with rapid stirring at room temperature. After that, the considered catalyst was separated by centrifuging and was washed with methanol for 5 min three times. Finally, the catalyst was dried at 30 °C. Other B-NPs (Pt/Fe and Pt/Pd) were synthesized in a similar manner. All the B-NPs were immediately black in color after 1 min from the addition of the hydrazine hydrate solution (as reducing agent). Then, all of these B-NPs were characterized by the FE-SEM analysis.

dx.doi.org/10.1021/cs300507a | *ACS Catal.* 2013, 3, 139−149

4.3.2. Preparation of the Pt/Pd/Fe T-NP. The Pt/Pd/Fe alloy NPs were obtained by mixing and stirring equal volumes of two microemulsion solutions in a beaker, one was an aqueous solution of metal salts, which was previously prepared by mixing three microemulsions with the content of 7×10^{-3} mmol of each of these metal salts stirring for 30 min, and the other was an aqueous solution of 0.9 mmol hydrazine hydrate. The corresponding reduction reactions can be expressed as (eqs 10−12):

$$Pt^{4+} + N_2H_5^+ + 5OH^- \rightarrow Pt^0 + N_2 + 5H_2O \quad (10)$$

$$2Pd^{2+} + N_2H_5^+ + 5OH^- \rightarrow 2Pd^0 + N_2 + 5H_2O \quad (11)$$

$$2Fe^{2+} + N_2H_5^+ + 5OH^- \rightarrow 2Fe^0 + N_2 + 5H_2O \quad (12)$$

The reaction time for mixing the two above-mentioned microemulsions was prolonged for 1 h with rapid stirring at room temperature to complete the reduction of metal ions. However, the change in the color of this NP from brownish-olive to black was immediately apparent in 1 min time. Subsequently, methanol was added to the beaker for phase separation. The mixture was centrifuged and the liquid phase was separated by decantation to get the catalyst, and in the following the catalyst was washed with methanol three times. Then, the catalyst was dried at 30 °C. Finally, the synthesized NPs were characterized by FE-SEM, TEM, XRD, and XRF analyses.

4.4. General Procedure of the Hydrodechlorination of Chlorobenzene. In a 25 mL two-necked flask, the mixture of chlorobenzene (5 mmol), ammonium formate (5 mmol), and the present nano-catalyst (5.7×10^{-4} mmol) was added in methanol (3 mL). The flask was sealed, and the mixture was allowed to stir at room temperature for the appropriate time. The reactions were monitored by thin layer chromatography (TLC). After the reaction was completed, the solid phase was separated by centrifuge and washed with water to remove salts from the catalyst. The remaining solution was then washed with acetone to remove adsorbed organic substrate. Finally, the prepared samples were analyzed by GC.

AUTHOR INFORMATION

Corresponding Author

*E-mail: Heshmatpour@kntu.ac.ir (F.H.), Balalaie@kntu.ac.ir (S.B.). Phone: (+9821) 23064230. Fax: (+9821) 22853650.

Notes

The authors declare no competing financial interest.

ACKNOWLEDGMENTS

The authors are grateful to K.N. Toosi University of Technology for the help to undertake this work.

REFERENCES

(1) Myneni, S. C. B. *Science* **2002**, *295*, 1039−1041.
(2) Lin, C.-T. *Prog. Org. Coat.* **2001**, *42*, 226−235.
(3) Fensterheim, R. J. *NLGI Spokesman* **2001**, *65*, 18−25.
(4) Morra, M. J.; Borek, V.; Koolpe, J. *J. Environ. Qual.* **2000**, *29*, 706−715.
(5) Eduljee, G. H., Hester, R. E., Harrison, R. M., Eds.; *Waste Incineration and the Environment*; Royal Society of Chemistry: Cambridge, U.K., 1994.
(6) Coq, B.; Ferrat, G.; Figueras, F. *J. Catal.* **1986**, *101*, 434−445.
(7) Lingaiah, N.; Babu, N. S.; Gopinath, R.; Reddy, P. S. S.; Prasad, P. S. S. *Catal. Surv. Asia* **2006**, *10*, 29−30.
(8) Wang, C. B.; Zhang, W.-X. *Environ. Sci. Technol.* **1997**, *31*, 2154−2156.
(9) Lien, H. L.; Elliott, D. W.; Sun, Y. P.; Zhang, W.-X. *J. Environ. Eng. Manage.* **2006**, *16*, 371−380.
(10) Morales, J.; Hutcheson, R.; Cheng, I. F. *J. Hazard. Mater.* **2002**, *90*, 97−108.
(11) Kim, Y. H.; Carraway, E. R. *Environ. Sci. Technol.* **2003**, *24*, 1455−1463.
(12) Matheson, L. J.; Tratnyek, P. G. *Environ. Sci. Technol.* **1994**, *28*, 2045−2053.
(13) Li, L.; Fan, M.; Brown, R. C.; Leeuwen, J. V.; Wang, J.; Wang, W.; Song, Y.; Zhang, P. *Crit. Rev. Environ. Sci. Technol.* **2006**, *36*, 405−431.
(14) Malinowski, A.; Juszczyk, W.; Bonarowska, M.; Pielaszek, J.; Karpinski, Z. *J. Catal.* **1998**, *177*, 153−163.
(15) Lingaiah, L. N.; Uddin, M. A.; Muto, A.; Sakata, Y. *Chem. Commun.* **1999**, 1657−1658.
(16) Zhang, W.-X. *J. Nanoparticle Res.* **2003**, *5*, 323−332.
(17) Liang, L.; Korte, N.; Goodlaxson, J. D.; Clausen, J.; Fernando, Q.; Muftikian, R. *Ground Water Monit. Rem.* **1997**, *17*, 122−127.
(18) Zhang, W.-X.; Wang, C.-B.; Lien, H.-L. *Catal. Today* **1998**, *40*, 387−395.
(19) Fürcht, Á.; Tungler, A.; Szabó, S.; Sárkány, A. *Appl. Catal., A* **2002**, *226*, 155−161.
(20) Carnevillier, C.; Epron, F.; Marecot, P. *Appl. Catal., A* **2004**, *275*, 25−33.
(21) Hermans, S.; Devillers, M. *Appl. Catal., A* **2002**, *235*, 253−264.
(22) Frank, B.; Emig, G.; Renken, A. *Appl. Catal., B* **1998**, *19*, 45−57.
(23) Homs, N.; Llorca, J.; Riera, M.; Jolis, J.; Fierro, J.-L. G.; Sales, J.; Ramírez de la Piscina, P. *J. Mol. Catal. A: Chem.* **2003**, *200*, 251−259.
(24) Carvalho, L. S.; Pieck, C. L.; Rangel, M. C.; Fígoli, N. S.; Grau, J. M.; Reyes, P.; Parera, J. M. *Appl. Catal., A* **2004**, *269*, 91−103.
(25) Carvalho, L. S.; Pieck, C. L.; Rangel, M. C.; Fígoli, N. S.; Vera, C. R.; Parera, J. M. *Appl. Catal., A* **2004**, *269*, 105−116.
(26) Balko, E. N.; Przybylski, E.; Von Tretini, F. *Appl. Catal., B* **1993**, *2*, 1−8.
(27) Hashimoto, Y.; Ayame, A. *Appl. Catal., A* **2003**, *250*, 247−254.
(28) Johnstone, R. A. W.; Wilby, A. H.; Entwistle, I. D. *Chem. Rev.* **1985**, *85*, 129−170.
(29) Cushing, B. L.; Kolesnichenko, V. L.; Oconnor, C. J. *Chem. Rev.* **2004**, *104*, 3893−3946.
(30) Yener, D. O.; Giesche, H. *J. Am. Ceram. Soc.* **2001**, *84*, 1987−1995.
(31) Fendler, J. H. *Chem. Rev.* **1987**, *87*, 877−899.
(32) Burda, C.; Chen, X.; Narayanan, R.; El-Sayed, M. A. *Chem. Rev.* **2005**, *105*, 1025−1102.
(33) Wang, W.; Huang, Q.; Liu, J.; Zou, Z.; Zhao, M.; Vogel, W.; Yang, H. *J. Catal.* **2009**, *266*, 156−163.
(34) Fouda-Onana, F.; Bah, S.; Savadogo, O. *J. Electroanal. Chem.* **2009**, *636*, 1−9.
(35) Ferrando, R.; Jellinek, J.; Johnston, R. L. *Chem. Rev.* **2008**, *108*, 845.
(36) Wanjala, B. N.; Fang, B.; Loukrakpam, R.; Chen, Y.; Engelhard, M.; Luo, J.; Yin, J.; Yang, L.; Shan, S.; Zhong, C.-J. *ACS Catal.* **2012**, *2*, 795.
(37) Yang, L.; Shan, S.; Loukrakpam, R.; Petkov, V.; Ren, Y.; Wanjala, B. N.; Engelhard, M. H.; Luo, J.; Yin, J.; Chen, Y.; Zhong, C.-J. *J. Am. Chem. Soc.* **2012**, *134*, 15048.
(38) Jellinek, J. *Faraday Discuss.* **2008**, *138*, 11.
(39) Adams, D. J.; Dyson, P. J.; Tavermer, S. J. *Chemistry in Alternative Reaction Media*; Wiley: Weinheim, Germany, 2003.
(40) Léger, B.; Nowicki, A.; Roucoux, A.; Rolland, J.-P. *J. Mol. Catal. A: Chem.* **2007**, *266*, 221−225.
(41) Wei, J.; Xu, X.; Liu, Y.; Wang, D. *Water Res.* **2006**, *40*, 348−354.
(42) Grittini, C.; Malcomson, M.; Fernando, Q.; Korte, N. *Environ. Sci. Technol.* **1995**, *29*, 2898−2900.
(43) He, F.; Zhao, D. *Appl. Catal., B* **2008**, *84*, 533−540.
(44) Zhou, T.; Li, Y.; Lim, T.-T. *Sep. Purif. Technol.* **2010**, *76*, 206−214.

(45) Frankel, K. A.; Jang, B. W.-L.; Roberts, G. W.; Spivey, J. J. *Appl. Catal., A* **2001**, *209*, 401−413.
(46) Ordonez, S.; Diez, F. W.; Sastre, H. *Appl. Catal., B* **2001**, *31*, 113−122.
(47) Nakao, R.; Rhee, H.; Uozumi, Y. *Org. Lett.* **2005**, *7*, 163−165.
(48) Giannoccaro, P.; Gargano, M.; Fanizzi, A.; Ferragina, C.; Leoci, A.; Aresta, M. *J. Mol. Cat. A: Chem.* **2005**, *227*, 133−140.
(49) Selvam, P.; Sonavane, S. U.; Mohapatra, S. K.; Jayaram, R. V. *Tetrahedron Lett.* **2004**, *45*, 3071−3075.
(50) Forni, P.; Prati, L.; Rossi, M. *Appl. Catal., B* **1997**, *14*, 49−53.
(51) Urbano, F. J.; Marinas, J. M. *J. Mol. Catal. A: Chem.* **2001**, *173*, 329−345.
(52) Aramendía, M. A.; Boráu, V.; García, I. M.; Jiménez, C.; Marias, J. M.; Urbano, F. J. *Appl. Catal., B* **1999**, *20*, 101−110.
(53) Hara, R.; Sato, K.; Sun, W.-H.; Takahashi, T. *Chem. Commun.* **1999**, 845−846.
(54) Liu, Y.; Schwartz, J. *Tetrahedron* **1995**, *51*, 4471−4482.
(55) Pinder, A. R. *Synthesis* **1980**, 425−452.
(56) Hites, R. A. *Acc. Chem. Res.* **1990**, *23*, 194−201.
(57) Aikawa, B.; Burk, R. C.; Sithole, B. B. *Appl. Catal., B* **2003**, *43*, 371−387.
(58) Xie, H.; Howe, J. Y.; Schwartz, V.; Monnier, J. R.; Williams, C. T.; Ploehn, H. J. *J. Catal.* **2008**, *259*, 111−122.
(59) Coq, B.; Cognion, J.-M.; Figueras, F.; Tournigant, D. *J. Catal.* **1993**, *141*, 21−33.
(60) Thompson, C. D.; Rioux, R. M.; Chen, N.; Ribeiro, F. H. *J. Phys. Chem. B* **2000**, *104*, 3067−3077.
(61) Jones, B. D.; Ingle, J. D. *Water Res.* **2005**, *39*, 4343−4354.
(62) Ukisu, Y.; Kameoka, S.; Miyadera, T. *Appl. Catal., B* **1998**, *18*, 273−279.
(63) Ukisu, Y.; Kameoka, S.; Miyadera, T. *Appl. Catal., B* **2000**, *27*, 97−104.
(64) Ghauch, A.; Assi, H. A.; Bdeir, S. *J. Hazard. Mater.* **2010**, *182*, 64−74.
(65) DeVor, R.; Carvalho-Knighton, K.; Aitken, B.; Maloney, P.; Holland, E.; Talalaj, L.; Elsheimer, S.; Clausen, C. A.; Geiger, C. L. *Chemosphere* **2009**, *76*, 761−766.
(66) Feng, J.; Lim, T.-T. *Chemosphere* **2005**, *59*, 1267−1277.
(67) Wang, C. B.; Zhang, W. X. *Environ. Sci. Technol.* **1997**, *31*, 2154−2156.